 CMES, vol.46, no.3, pp.209-220, 2009

Modeling and Solution for Gas Penetration of Gas-Assisted Injection Molding Based on Perturbation Method

Huamin Zhou[1], **Hua Zhang and Dequn Li**[2]

Abstract: Gas-assisted injection molding is an innovative process to manufacture hollow polymeric products, in which gas penetration is the primary and key problem. An analytical solution of the gas penetration interface is presented, based on perturbation method. First, the governing equations and boundary conditions are transformed to be dimensionless, where Capillary number Ca is introduced. Then matching asymptotic expansion method is applied to solve these equations, by using Ca and as perturbation parameters to get the inner and outer solutions, respectively. By matching these two solutions, the analytical model of gas penetration is obtained.

Keywords: Gas-assisted injection molding, gas penetration, perturbation method.

1 Introduction

Gas-assisted injection molding (GAIM) is an innovative process to manufacture hollow polymeric products, which comprises a partial injection of polymer melt into the mold cavity, followed by an injection of compressed gas. The gas penetrates into the polymer melt and forces it to fill the whole mold cavity. The process has inherent advantages of producing less warpage tendency and better surface quality with less polymer material and lower pressure and can be used to manufacture large and thick parts or parts which have thick and thin sections [Avery (2000); Parvez, Ong, and Lam (2002); Zheng, Yang, Yang, Chen, Li, and Shen (2008)].

However, because gas-assisted injection molding process involves dynamic interaction between two dramatically dissimilar materials flowing within cavities, the product, tool and process designs for GAIM are quite complicated. Further, previous experience with conventional injection molding is no longer sufficient to deal

[1] Corresponding author.
[2] State Key Laboratory of Materials Processing and Mold Technology, Huazhong University of Science and Technology,Wuhan, The People's Republic of China

with this process, especially in designing the gas-channel network and optimizing the processing window. So the modeling and simulation of the GAIM process are needed urgently.

Gas penetration is the primary and key problem of gas-assisted injection molding, which makes melt flow more complex. Besides, in the filling simulation of GAIM, the melt filling in the thin cavity is assumed as Hele-Shaw flow which is similar to conventional injection molding, while the gas penetration interface should be solved simultaneously and considered as boundary conditions [Marcilla, Odjo-Omoniyi, Ruiz-Femenia, and García-Quesada (2006); Chen, Li, Zhou, Li, He, and Tang, (2008)]. Chen *et al.* used heat transfer parameters to set the thickness of the stagnant material behind the advancing gas front [Chen, Hsu, and Hsu (1995)]. Yang *et al.* studied the effect of the gas-channel dimension on gas penetration [Yang, Huang, and Liau (1996)]. Huzyak and Koellin studied isothermal gas penetration of Newtonian melts in circular tubes by experiments [Huzyak, and Koelling (1997)]. Chau presented a generalized Newtonian model to predict the three-dimensional gas penetration phenomenon [Chau (2008)]. Li and Isayev put forward a physical model for the gas/melt front based on interface kinematics and dynamics [Li, and Isayev (2004)].

Although some investigations have focused on gas penetration of gas-assisted injection molding, most existing studies are based on empirical and experimental approaches. There is still lack of exact and reasonable analytical model that can be adopted directly in analysis and simulation. In this paper, a mathematical model governing the behavior of gas penetration is established, followed by a thorough solution based on the matching asymptotic expansion method. In the deduction, the governing equations and boundary conditions are transformed to be dimensionless first. In the meantime, Capillary number Ca is introduced into the dimensionless equations. Then matching asymptotic expansion method is applied to solve these equations. Ca and $Ca^{2/3}$ are used as perturbation parameters to get the inner and outer solutions of gas penetration interface, respectively. By matching these two solutions, the analytical model of gas penetration thickness ratio is obtained.

2 Modeling of the process

As shown in Fig. 1, gas-assisted injection molding involves the injection of a short shot of polymer into the cavity. When gas is introduced into the molten material, it takes the path of least resistance into areas of the part with low pressure and high temperature. As the gas penetrates through the part, it cores out thick sections by displacing the polymer melt. This polymer melt fills out the rest of the cavity. After cooled down, the part is ejected by opening the mold.

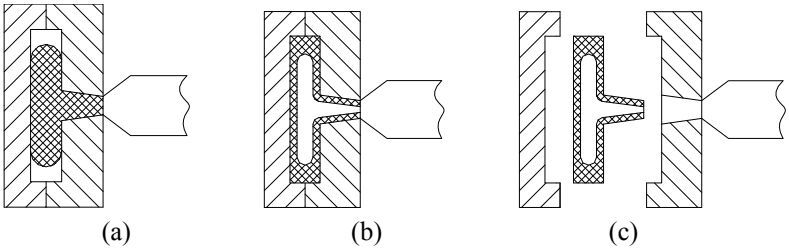

Figure 1: Schematic diagram for gas-assisted injection molding process: (a) short shot of polymer; (b) gas penetration; (c) ejection after cooled down

During the stage of gas penetration, the gas bubble follows the "path of least resistance". To induce the gas bubble to proceed in the desired path, it is essential to design gas channel, that is, a rib with thicker section of a part, as shown in Fig. 2. A channel with thick section will usually be of lower pressure and higher temperature than thinner areas.

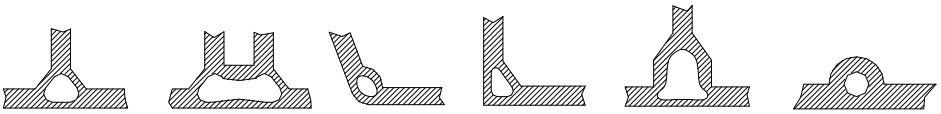

Figure 2: Typical gas channel geometries

The gas penetration in the gas channel is the most important and complicated problem of GAIM. As shown in Fig. 3, four distinct flow regions can be identified in gas penetration: the solid frozen layer of polymer close to the mold wall, the deforming viscous polymer melt, the penetration gas, and the unfilled cavity. These four regions are confined by the melt and gas fronts. The melt flow front is identical to that in conventional injection molding. The gas penetration and its interface are responsible for transmitting the pressure required to move the viscous melt.

Penetration is a common phenomenon in engineering [Ma, Zhang, Lian, and Zhou (2009); Wang, Zhang, Gao, and Wang (2007)]. The gas penetration interface is a very complicated problem, with features of non-linearity, variable coefficients, and complex boundary conditions. It is difficult to obtain exact analytical solution for this interface. In recent years, as an approximate approach, the perturbation method has undergone rapid developments and achieved exciting advancements [Lee, Lu, and Liu (2008); Lu, and Zhu (2007)]. In this paper, the matching asymptotic ex-

pansion method [Marin (2008); Sarkar, and Sonti (2007)] is used to solve the gas penetration interface, which is a kind of parametric perturbation methods. Its basic idea is to use more than one asymptotic expansion for the problem. Each expansion is effective in partial areas and adjacent areas have overlapping regions. Therefore, these expansions would accord with each other through matching in the overlapping regions.

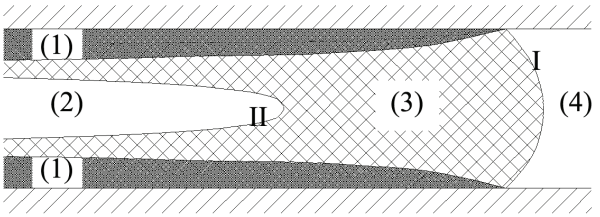

Figure 3: Schematic notation for flow regions and their interface in the gas penetration, where (1) the solid frozen layer of polymer, (2) the penetration gas, (3) the deforming viscous polymer melt, (4) the unfilled cavity; (I) the polymer melt front, (II) the gas front

3 Solution of the gas penetration

The melt filling is assumed as Hele-Shaw flow. Because the viscosity of polymer melt is sufficiently high, the inertia and transients can be neglected. As shown in Fig. 4(a), suppose the gas penetrates into the melt in x direction with the penetration thickness ratio being β. And $\vec{n} = n_x\vec{i} + n_y\vec{j} + n_z\vec{k}$ and $\vec{t} = t_x\vec{i} + t_y\vec{j} + t_z\vec{k}$ represent the inner normal and tangent vector, respectively. The governing equations and boundary conditions in the gas penetration interface can be simplified as

$$\frac{\partial u}{\partial x} + \frac{\partial w}{\partial z} = 0 \tag{1a}$$

$$-\frac{\partial P}{\partial x} + \eta\left(\frac{\partial^2 u}{\partial x^2} + \frac{\partial^2 u}{\partial z^2}\right) = 0 \tag{1b}$$

$$-\frac{\partial P}{\partial z} + \eta\left(\frac{\partial^2 w}{\partial x^2} + \frac{\partial^2 w}{\partial z^2}\right) = 0 \tag{1c}$$

$$(u - U)n_x + wn_z = 0 \tag{2a}$$

$$\frac{\partial u}{\partial x}t_x n_x + \frac{1}{2}\left(\frac{\partial u}{\partial z} + \frac{\partial w}{\partial x}\right)(t_x n_z + t_z n_x) + \frac{\partial w}{\partial z}t_z n_z = 0 \tag{2b}$$

$$P-2\eta[\frac{\partial u}{\partial x}n_x^2+(\frac{\partial u}{\partial z}+\frac{\partial w}{\partial x})n_x n_z+\frac{\partial w}{\partial z}n_z^2]=P_0-\frac{T}{R} \tag{2c}$$

where U is the gas penetration velocity in x direction, P_0, T, R are the pressure of the gas, the melt surface tension coefficient and the curvature radius of the gas penetration interface respectively.

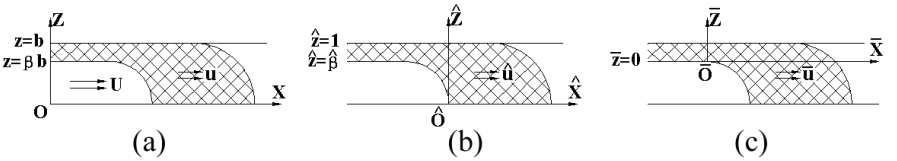

Figure 4: Illustrative for: (a) gas penetration in the channel; (b) the outer coordinate system; (c) the inner coordinate system

3.1 Outer solution

An outer coordinate system for the gas-melt interface is set up as Fig. 4(b), and the dimensionless variables in this system are defined by $\hat{x}=\frac{x-Ut}{b}$, $\hat{z}=\frac{z}{b}$, $\hat{R}=\frac{R}{b}$, $\hat{u}=\frac{u-U}{U}$, $\hat{w}=\frac{w}{U}$, and $\hat{P}=\frac{P-P_0}{T/b}$.

Based on the above variables, dimensionless transforms of Eqs. (1) and (2) result in

$$\frac{\partial u}{\partial x}+\frac{\partial w}{\partial z}=0 \tag{3a}$$

$$\frac{\partial P}{\partial x}=Ca(\frac{\partial^2 u}{\partial x^2}+\frac{\partial^2 u}{\partial z^2}) \tag{3b}$$

$$\frac{\partial P}{\partial z}=Ca(\frac{\partial^2 w}{\partial x^2}+\frac{\partial^2 w}{\partial z^2}) \tag{3c}$$

$$un_x+wn_z=0 \tag{4a}$$

$$\frac{\partial u}{\partial x}t_x n_x+\frac{1}{2}(\frac{\partial u}{\partial z}+\frac{\partial w}{\partial x})(t_x n_z+t_z n_x)+\frac{\partial w}{\partial z}t_z n_z=0 \tag{4b}$$

$$P-2Ca[\frac{\partial u}{\partial x}n_x^2+(\frac{\partial u}{\partial z}+\frac{\partial w}{\partial x})n_x n_z+\frac{\partial w}{\partial z}n_z^2]=-\frac{1}{R} \tag{4c}$$

where $Ca=\eta U/T$ is Capillary number. For convenience, the superscripts of the variables are removed.

Suppose that the gas penetration interface is denoted by $z = h(x)$, and hence $\frac{dz}{dx} = \frac{dh}{dx} = \frac{t_z}{t_x} = -\frac{n_x}{n_z}$. Combining with boundary conditions, it follows that

$$P = -Ca[2\frac{\partial u}{\partial x} + \frac{dh}{dx}(\frac{\partial u}{\partial z} + \frac{\partial w}{\partial x})] + \frac{d^2h}{dx^2}[1 + (\frac{dh}{dx})^2]^{-3/2} \tag{5}$$

Adopting Ca as perturbation parameter, considering governing equations and boundary conditions while $Ca \to 0$ with the perturbation theory, the approximation function of h in the outer coordinate system can be obtained as

$$-1 = \frac{d^2h^0}{dx^2}[1 + (\frac{dh^0}{dx})^2]^{-3/2} \tag{6}$$

By further inference, it results in

$$h^0(x) = \sqrt{1 - (x+1)^2} \tag{7}$$

Eq. (7) is the outer solution of the gas penetration interface.

3.2 Inner solution

The point of intersection between the mold wall and the gas perturbation interface determined by outer solution is the inconsistent region of the outer solution. This point is selected as origin to set up the inner coordinate system (as shown in Fig. 4(c)). In this inner coordinate system, the variables are magnified by δ with $\delta = Ca^m$. In order to ensure that the magnified equations are in balance and as simple as possible, m prefers to be 2/3 and

$$\begin{aligned} &\bar{d} = \frac{1-\beta}{\delta}, \quad \bar{x} = \frac{x+1}{\delta^{1/2}}, \quad \bar{z} = \frac{z-1}{\delta}, \quad \bar{h} = \frac{h-1}{\delta}, \\ &\bar{u} = u, \quad \bar{w} = \frac{w}{\delta^{1/2}}, \quad \bar{P} = P \end{aligned} \tag{8}$$

Substituting Eq. (8) into Eqs. (3) and (4), the resulting governing equations and boundary conditions in inner coordinate system can be write as

$$\frac{\partial \bar{u}}{\partial \bar{x}} + \frac{\partial \bar{w}}{\partial \bar{z}} = 0 \tag{9a}$$

$$\frac{\partial \bar{P}}{\partial \bar{x}} = \delta \frac{\partial^2 \bar{u}}{\partial \bar{x}^2} + \frac{\partial^2 \bar{u}}{\partial \bar{z}^2} \tag{9b}$$

$$\frac{\partial \bar{P}}{\partial \bar{z}} = \delta^2 \frac{\partial^2 \bar{w}}{\partial \bar{x}^2} + \delta \frac{\partial^2 \bar{w}}{\partial \bar{z}^2} \tag{9c}$$

$$\bar{w} = \frac{d\bar{h}}{d\bar{x}}\bar{u} \tag{10a}$$

$$(\frac{\partial \bar{u}}{\partial \bar{z}} + \delta\frac{\partial \bar{w}}{\partial \bar{x}})[1-\delta(\frac{d\bar{h}}{d\bar{x}})^2] - 4\delta\frac{\partial \bar{u}}{\partial \bar{x}}\frac{d\bar{h}}{d\bar{x}} = 0 \tag{10b}$$

$$\bar{P} = -2\delta\frac{\partial \bar{u}}{\partial \bar{x}} - (\delta\frac{\partial \bar{u}}{\partial \bar{z}} + \delta^2\frac{\partial \bar{w}}{\partial \bar{x}})\frac{d\bar{h}}{d\bar{x}} + \frac{d^2\bar{h}}{d\bar{x}^2}[1+\delta(\frac{d\bar{h}}{d\bar{x}})^2]^{-\frac{3}{2}} \tag{10c}$$

Considering Eqs. (9) and (10) while $\delta \to 0$ with the perturbation theory, the approximation function of $\bar{h}$ in the inner coordinate system can be obtained as

$$\frac{\partial^3 \bar{h}^0}{\partial \bar{x}^3} = \frac{-3(\bar{h}^0 + \bar{d})}{(\bar{h}^0)^3} \tag{11}$$

Employ fourth-order Runge-Kutta method to solve the asymptotic expansion of Eq. (11) [Lee, and Liu (2009); Liu, and Atluri (2009)], resulting in

$$\bar{h}^0(\bar{x}) \approx \frac{A_2 \times 3^{2/3}(\bar{x}+\bar{x}_0)^2}{\bar{d}} + A_1 \times 3^{1/3}(\bar{x}+\bar{x}_0) + A_0 \times \bar{d} + O(\frac{1}{\bar{x}}) \tag{12}$$

where $A_2 = -0.3215, A_1 = -0.096, A_0 = -2.9$.

Eq. (12) is the inner solution of the gas penetration interface.

3.3 Matching

According to the matching asymptotic expansion theory, the inner solution when $\bar{x} \to -\infty$ might match the outer solution when $x \to -1$. This match is satisfied in any coordinate system, and here the outer coordinate system is selected. Inverse transformation to the inner solution according to Eq. (8) results in

$$\begin{aligned} h^0(x) \approx & 1 + \frac{A_2 \times 3^{2/3}(x+1)^2}{\bar{d}} + \delta^{1/2}(\frac{2 \times A_2 \times 3^{2/3}\bar{x}_0}{\bar{d}} + A_1 \times 3^{1/3})(x+1) \\ & + \delta(\frac{A_2 \times 3^{2/3}\bar{x}_0^2}{\bar{d}} + A_1 \times 3^{1/3}\bar{x}_0 + A_0 \times \bar{d}) + \cdots\cdots \end{aligned} \tag{13}$$

While $x \to -1$, the outer solution Eq. (7) can be expanded as

$$h^0(x) \approx 1 - \frac{1}{2}(x+1)^2 + O((x+1)^4) \tag{14}$$

Eqs. (13) and (14) must match each other. Because $(x+1)^n$ series are linearly independent of each other, the coefficients of $(x+1)^n$of the two solutions should be equivalent. Therefore, $\bar{d}$can be obtained as

$$\bar{d} = -2A_2 \times 3^{2/3} = 1.3375 \tag{15}$$

Consequently, the gas penetration thickness ratio in steady penetration region is calculated by

$$\beta = 1 - \delta\bar{d} = 1 - 1.3375Ca^{2/3} \tag{16}$$

3.4 Correction

Eq. (16) is the deduced gas penetration thickness ratio calculating model. And yet this calculation will lead to serious deviation when Ca becomes larger. The reason is the following two: (a) perturbation method has close approximation only round the perturbation point. Perturbation parameter Ca has been confined by $Ca \to 0$ and $Ca^{2/3} \to 0$ in the deduction process, as a result the deduced solution only suits for little value of Ca; (b) higher-order items of the asymptotic expansion of the gas penetration interface solution have been neglected, which would lower the accuracy. In order to make the educed model applicable to a larger range of Ca, a reasonable correction is necessary.

Suppose that the correction function of gas penetration in outer coordinate system is expressed by

$$h(x) \approx \beta - De^{kx} \tag{17}$$

where D, k are constants needed to be obtained.

According to the no slip condition at the mold wall, the velocity and pressure can be defined by

$$u(x,z) \approx -1 + e^{kx} f_1(z) + O(e^{2kx}) \tag{18a}$$

$$w(x,z) \approx e^{kx} f_2(z) + O(e^{2kx}) \tag{18b}$$

$$P(x,z) \approx Cae^{kx} f_3(z) + O(e^{2kx}) \tag{18c}$$

where $f_1, f_2, f_3$are functions to be solved.

Apply Eqs. (17) and (18) to the governing and boundary conditions equations, and make f_2 expressed as an assembly of trigonometric functions. With that, the simultaneous equations with respect to all educible constants can be obtained. And these constants will be calculated by solving these equations.

4 Verification

The experiment carried out by GE Corporate Research and Development [Poslinski, Oehler, and Stokes, (1995)] is employed for verification. This experiment studied the gas penetration in transparent tubes in different conditions so as to investigate the factors affecting the penetration. A schematic diagram of the apparatus used in the experiment is shown in Fig. 5.

Experiments were performed using 26-cm-long disposable tubes of different inner radii: 3.83-mm radius plastic pipettes, and rigid PVC tubing with radii of 2.95, 4.76 and 6.32 mm. The pipettes and PVC tubes were marked with a graded scale to facilitate location of the gas and melt fronts. A video camera speed of 30 frames/s was used to record the gas and melt fronts during the penetration. The thickness of the cured skin was measured by using a nondestructive Hall-effect approach, having an accuracy of ± 0.01 mm. Two translucent liquids, RTV-108 and RTV 118 (both from General Electric), were used in experiments.

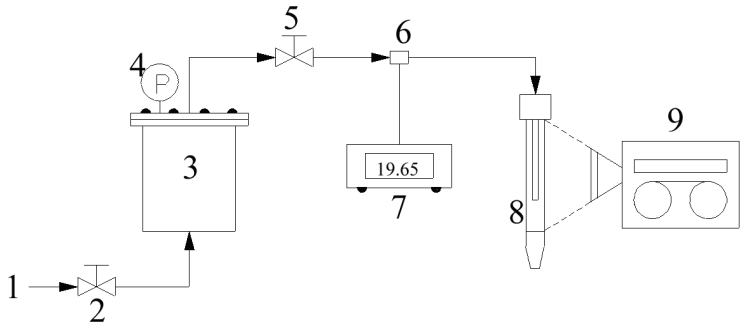

Figure 5: Schematic diagram of the experimental apparatus, where (1) air supply, (2) control valve, (3) pressurized gauge, (4) manometer, (5) control valve, (6) pressure transducer, (7) digital readout, (8) transparent tube assembly, (9) video camera

The experimental and calculated data of the skin melt thickness ratio are compared in Fig. 6. The initial calculation of the skin melt thickness ratio is $d = 1.3375Ca^{2/3}$, and this initial value is corrected by the temporal governing equations and boundary conditions. From Fig. 6, it can be seen that:

(a) all the curve lines show that Capillary number is the key factor determining the skin melt thickness ratio, and Capillary number synthesizes the influence of the gas penetration velocity, viscosity and surface tension of the melt, and other processing parameters;

(b) the three curve lines reflect that the skin melt thickness ratio increases with Capillary number largening;

(c) while the Capillary number is less than 10^{-2}, the initial calculation without correction agrees well with the experiment result, but it will lead to large errors when the Capillary number exceeds 10^{-2};

(d) after correction, the calculation is closer to the experiment in a wider range, sufficient for the engineering design.

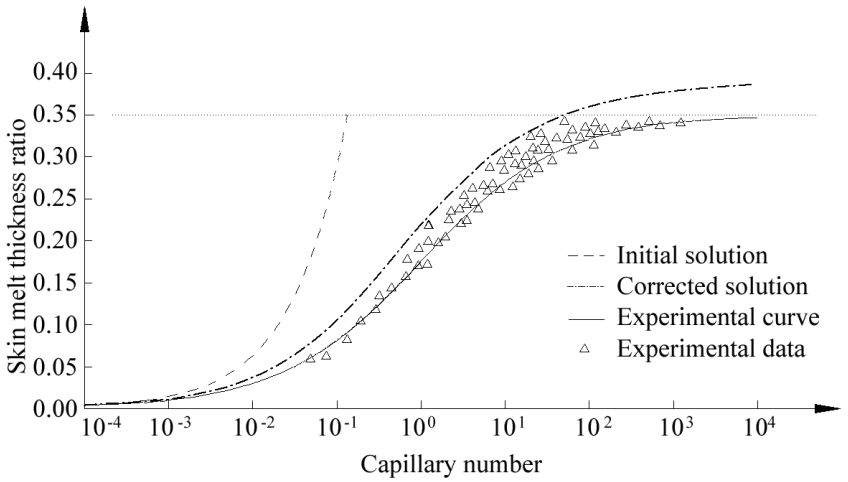

Figure 6: The skin melt thickness ratio versus the Capillary number

5 Conclusion

The modeling and solution of gas penetration in gas-assisted injection molding is presented in this paper. By applying the matching asymptotic expansion method, an approximated analytical model for gas penetration is deduced. The comparisons with experiments show that the initial calculation agrees well with the experimental result for small Capillary number, and the calculation after correction is closer to the experiment in a wider range.

Acknowledgement The authors would like to acknowledge financial support from the National Natural Science Foundation Council of the People's Republic of China (Grant No.: 50675080, 50875095).

References

Avery, J. (2000): Gas-assist injection molding: principles and applications, Cincinnati: Hanser Gardner Publications, Inc.

Chau, S.W. (2008): Three-dimensional simulation of primary and secondary penetration in a clip-shaped square tube during a gas-assisted injection molding process. *Polymer Engineering and Science*, vol. 48, no. 9, pp. 1801-1814.

Chen, L.; Li, J.; Zhou, H.; Li, D.; He, Z.; Tang, Q. (2008): A study on gas-assisted injection molding filling simulation based on surface model of a contained circle channel part. *Journal of Materials Processing Technology*, vol. 208, no. 1-3, pp. 90-98.

Chen, S.C.; Hsu, K.F.; Hsu, K.S. (1995): Analysis and experimental study of gas penetration in a gas-assisted injection-molded spiral tube. *Journal of Applied Polymer Science*, vol. 58, no. 4, pp. 793-799.

Huzyak, P.C.; Koelling, K.W. (1997): Penetration of a long bubble through a viscoelastic fluid in a tube. *Journal of Non-Newtonian Fluid Mechanics*, vol. 71, no. 1-2, pp. 73-88.

Lee, H.C.; Liu, C.S. (2009): The fourth-order group preserving methods for the integrations of ordinary differential equations. *CMES: Computer Modeling in Engineering and Science*, vol. 41, no. 1, pp. 1-26.

Lee, S.Y.; Lu, S.Y.; Liu, Y.R. (2008): Exact large deflection solutions for timoshenko beams with nonlinear boundary conditions. *CMES: Computer Modeling in Engineering and Science*, vol. 33, no. 3, pp. 293-312.

Li, C.T.; Isayev, A.I. (2004): Primary and secondary gas penetration during gas-assisted injection molding. Part I: Formulation and modeling. *Polymer Engineering and Science*, vol. 44, no. 5, pp. 983-991.

Liu, C.S.; Atluri, S.N. (2009): A highly accurate technique for interpolations using very high-order polynomials, and its applications to some ill-posed linear problems. *CMES: Computer Modeling in Engineering and Science*, vol. 43, no. 3, pp. 253-276.

Lu, Y.Y.; Zhu, J.X. (2007): Perfectly matched layer for acoustic waveguide modeling - benchmark calculations and perturbation analysis. *CMES: Computer Modeling in Engineering and Science*, vol. 22, no. 3, pp. 235-247.

Ma, S.; Zhang, X.; Lian, Y.P.; Zhou X. (2009): Simulation of high explosive explosion using adaptive material point method. *CMES: Computer Modeling in Engineering and Science*, vol. 39, no. 2, pp. 101-123.

Marcilla, A.; Odjo-Omoniyi, A.; Ruiz-Femenia, R.; García-Quesada, J.C. (2006): Simulation of the gas-assisted injection molding process using a mid-plane model of a contained-channel part. *Journal of Materials Processing Technology*, vol. 178, no. 1-3, pp. 350-357.

Marin, L. (2008): Stable MFS solution to singular direct and inverse problems associated with the Laplace equation subjected to noisy data. *CMES: Computer Modeling in Engineering and Science*, vol. 37, no. 3, pp. 203-242.

Parvez, M.A.; Ong, N.S.; Lam, Y.C.; Tor, S.B. (2002): Gas-assisted injection

molding: the effects of process variables and gas channel geometry. *Journal of Materials Processing Technology*, vol. 121, no. 1, pp. 27-35.

Poslinski, A.J.; Oehler, P.R.; Stokes, V.K. (1995): Isothermal gas-assisted displacement of viscoplastic liquids in tubes. *Polymer Engineering and Science*, vol. 35, no. 11, pp. 877-892.

Sarkar, A.; Sonti, V.R. (2007): Asymptotic analysis for the coupled wavenumbers in an infinite fluid-filled flexible cylindrical shell: The axisymmetric mode. *CMES: Computer Modeling in Engineering and Science*, vol. 21, no. 3, pp. 193-207.

Wang, L.; Zhang, S.; Gao, W.M.; Wang, X. (2007): FEM analysis of knife penetration through woven fabrics. *CMES: Computer Modeling in Engineering and Science*, vol. 20, no. 1, pp. 11-20.

Yang, S.Y.; Huang, F.Z.; Liau, W.N. (1996): A study of rib geometry for gas-assisted injection molding. *Polymer Engineering and Science*, vol. 36, no. 23, pp. 2824-2831.

Zheng, G.Q.; Yang, W.; Yang, M.B.; Chen, J.B.; Li, Q.; Shen, C.Y. (2008): Gas-assisted injection molded polypropylene: the skin-core structure. *Polymer Engineering and Science*, vol. 48, no. 5, pp. 976-986.